The 2011 World Congress on
Advances in Structural Engineering and Mechanics (ASEM'11+)
Seoul, Korea, 18-22 September, 2011

Testing of Ferritic Stainless Steel Tubular Structural Elements

*S. Afshan [1)] and L. Gardner [2)]

[1), 2)] *Department of Civil and Environmental Engineering, Imperial College London, UK*
[1)] *sheida.afshan06@imperial.ac.uk*
[2)] *leroy.gardner@imperial.ac.uk*

ABSTRACT

Stainless steel is gaining increasing usage in construction owing to its durability, favourable mechanical properties and its aesthetic appearance, with the austenitic grades being the most commonly utilised. Austenitic stainless steels have a high nickel content (8%-11%), resulting in high initial material cost and significant price fluctuations; this, despite its desirable properties, represents a considerable disadvantage in terms of material selection. Ferritic stainless steels, having no or very low nickel content, may offer a more viable alternative for structural applications, reducing both the level and variability of the initial material cost. In comparison to the most widely used austenitic grades, the ferritic grades typically have higher yield strengths (250-350 N/mm^2) and are easier to machine and work. Furthermore, by varying the chromium content (10.5%-29%), and with additions of other alloying elements, the required corrosion resistance for a wide range of structural applications and operating environments can be achieved. There is currently limited information available on the structural performance of this type of stainless steel. Therefore, to overcome this limitation, a series of material and cross-section tests have been performed, covering both the standard 1.4003 grade and the 1.4509 grade, which has improved weldability and corrosion resistance. The experimental results are reported, analysed and compared to the results of tests performed on other stainless steel grades. Finally, design recommendations suitable for incorporation into Eurocode 3: Part 1.4 (2006) have been proposed.

1. INTRODUCTION

The physical and mechanical characteristics of stainless steel such as high strength, stiffness and ductility, weldability, durability, good fire resistance and ready re-use and recycling make it suitable for a number of architectural and structural applications. The austenitic, EN 1.4301 and 1.4401, stainless steel grades, containing 17–18% chromium and 8–11% nickel, are most commonly used in construction. Both grades have minimum specified design strength (0.2% proof strength) of 210-240 N/mm^2 (EN 10088-4 2009). The high nickel content of the austenitic grades provides a number of positive attributes, such as very good ductility and elevated temperature performance, but the initial material cost is high, which is a significant disincentive for material selection.

Ferritic stainless steels, having no or very low nickel content, may offer a more viable alternative for structural applications, due to their lower initial material cost and improved price

stability. The main alloying element is chromium, with contents typically between 11 and 18% (EN 10088-4 2009). These steels are easier to work and machine than the austenitic grades and have higher annealed yield strength of 250-350 N/mm^2. Furthermore, by varying the chromium content (10.5%-29%), and with additions of other alloying elements, the required corrosion resistance for a wide range of structural applications and operating environments can be achieved. Stabilised ferritic grades, with additions of titanium and niobium alloying elements, such as EN 1.4509 and 1.4521 are broadly similar in terms of corrosion resistance to the EN 1.4301 and 1.4401 austenitic grades.

Ferritic stainless steel has been widely used in various applications in the automotive industry, road and rail transport, power generation and mining while its structural usage has remained relatively scarce. Despite inclusion of the three traditional ferritic grades (EN 1.4003, 1.4016 and 1.4512) in Eurocode 3: Part 1.4 (2006), their structural performance is largely unverified. This is mainly due to the lack of test data on ferritic stainless steel relevant to construction applications, with no data available on the new ferritic grades included in the EN 10088-4 (2009) stainless steel material standard. Hence, the focus of the present paper is to describe a comprehensive laboratory testing programme on grades 1.4003 and 1.4509 stainless steel square and rectangular hollow sections, which has been recently conducted at Imperial College London. Eight stub column tests and eight beam tests, including 3-point bending and 4-point bending configurations, have been carried out. A total of 20 material tests, covering tensile flat and corner coupons, have also been performed. The experimental results obtained are reported, analysed and compared to the results of tests performed on other stainless steel grades. Finally, design recommendations suitable for incorporation into Eurocode 3: Part 1.4 (2006) have been proposed.

2. EXPERIMENTAL PROGRAMME

2.1. Introduction

A laboratory testing programme comprising material tests, stub column tests and 3-point and 4-point bending tests has been conducted at Imperial College London to investigate the structural performance of ferritic stainless steel tubular structural elements. Four section sizes were employed for all tests, namely RHS 120×80×3, RHS 60×40×3, SHS 80×80×3 and SHS 60×60×3. The first three sections were of the standard 1.4003 grade, while the SHS 60×60×3 was grade 1.4509, which has improved weldability and corrosion resistance. The chemical compositions and the tensile properties of the coil material from which the specimens were formed, as provided by the mill certificates, are presented in Tables 1 and 2 respectively. No chemical composition details were available for the SHS 60×60×3. The notation employed in Table 2 is as follows: $\sigma_{0.2}$ is the 0.2% proof stress, $\sigma_{1.0}$ is the 1% proof stress, σ_u is the ultimate tensile stress and ε_f is the tensile strain at fracture.

Table 1. Chemical composition of grade EN 1.4003 stainless steel specimens

Section	C (%)	Si (%)	Mn (%)	P (%)	S (%)	Cr (%)	Ni (%)	N (%)
RHS 120×80×3	0.005	0.50	1.44	0.029	0.002	11.30	0.40	0.01
RHS 60×40×3	0.010	0.37	1.46	0.029	0.003	11.20	0.50	0.01
SHS 80×80×3	0.010	0.25	1.43	0.028	0.003	11.30	0.40	0.01

Table 2. Mechanical properties as stated in the mill certificates

Section	$\sigma_{0.2,mill}$ (N/mm^2)	$\sigma_{1.0,mill}$ (N/mm^2)	$\sigma_{u,mill}$ (N/mm^2)	ε_f (%)
RHS 120×80×3	346	368	498	42
RHS 60×40×3	339	360	478	38
SHS 80×80×3	321	343	462	45

2.2. Material tests

Material tests were conducted to determine the basic engineering stress-strain response of the SHS and RHS ferritic specimens. All material was extracted from the same lengths of tube as the beam and the stub column specimens. Parallel necked coupons, each with a neck length of 150 mm and width of 20 mm, were machined from each of the four faces of the SHS and RHS specimens, resulting in a total of 16 tensile coupon tests. Stainless steel exhibits pronounced strain hardening, resulting in the corner regions of cold-formed sections having 0.2% proof strengths higher than that of the flat material (Ashraf et al. 2005). In order to investigate the extra degree of strength that is achieved in the cold-worked corner regions, tensile tests on corner coupons, with nominal length of 320 mm, extracted from the curved portions of each of the cold-formed sections were also conducted. The tests were performed using an Instron 8802 250 kN hydraulic testing machine, in accordance with EN 10002-1 (2000). Strain control was used to drive the testing machine at a strain rate of 0.002 %/s up to the 0.2% proof stress and 0.005 %/s until fracture. Static loads were obtained at key stages by holding the cross head of the testing machine for a duration of 2 minutes to allow stress relaxation to take place (see Fig. 1).

The obtained material data for each specimen is given in Table 3, whereas the weighted average (based on face width) tensile material properties of each section are given in Table 4. The specimen designation begins with the section size, e.g. SHS 80×80×3, followed by the test type - TF for tensile flat and TC for tensile corner- and finally the section face number 1, 2, 3 and 4 as explained in Fig. 2 (Face 1 contained the weld). The material parameters reported in Tables 3 and 4 are the Young's modulus E, the static 0.2% proof stress $\sigma_{0.2}$, the static 1% proof stress $\sigma_{1.0}$, the static ultimate tensile stress σ_u and the plastic strain at fracture ε_f (based on elongation over the standard gauge length $5.65\sqrt{A}$, where A is the cross-sectional area of the coupon). The measured stress-strain curves, up to 1% tensile strain, are depicted in Fig. 3.

Table 3. Coupon test results for each specimen

Specimen reference	E (N/mm^2)	$\sigma_{0.2}$ (N/mm^2)	$\sigma_{1.0}$ (N/mm^2)	σ_u (N/mm^2)	ε_f (%)
RHS 120×80×3-TF 1	210000	450	472	477	33
RHS 120×80×3-TF 2	220000	385	405	443	40
RHS 120×80×3-TF 3	230000	390	413	458	40
RHS 120×80×3-TF 4	220000	510	-[a]	535	23
RHS 120×80×3-TC	235000	535	-[a]	549	13
RHS 60×40×3-TF 1	225000	438	-[a]	460	18
RHS 60×40×3-TF 2	225000	455	-[a]	481	28
RHS 60×40×3-TF 3	220000	435	-[a]	440	32
RHS 60×40×3-TF 4	210000	450	-[a]	483	21
SHS 80×80×3-TF 1	220000	435	-[a]	440	36
SHS 80×80×3-TF 2	200000	425	435	447	36
SHS 80×80×3-TF 3	210000	400	418	432	38
SHS 80×80×3-TF 4	210000	465	-[a]	470	31
SHS 80×80×3-TC	240000	512	-[a]	520	11
SHS 60×60×3-TF 1	220000	510	-[a]	538	14
SHS 60×60×3-TF 2	220000	485	-[a]	493	20
SHS 60×60×3-TF 3	230000	500	-[a]	513	19
SHS 60×60×3-TF 4	210000	520	-[a]	537	13
SHS 60×60×3-TC	225000	580	-[a]	665	13

Note: [a] ultimate tensile stress preceded the 1% proof stress

Table 4. Weighted average tensile flat material properties

Specimen reference	E (N/mm^2)	$\sigma_{0.2}$ (N/mm^2)	σ_u (N/mm^2)	ε_f (%)
RHS 120×80×3	221100	423	472	34
RHS 60×40×3	220700	445	465	24
SHS 80×80×3	210000	431	447	35
SHS 60×60×3	220000	504	520	16

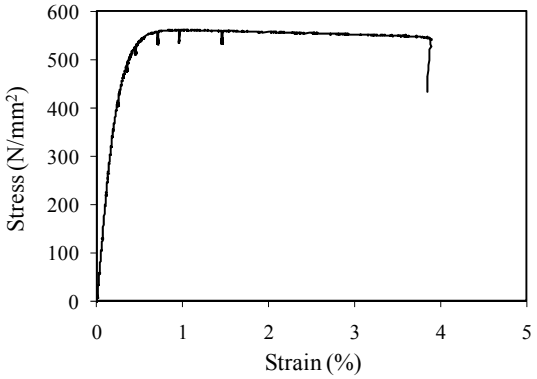

Fig. 1. Typical measured tensile stress-strain curve

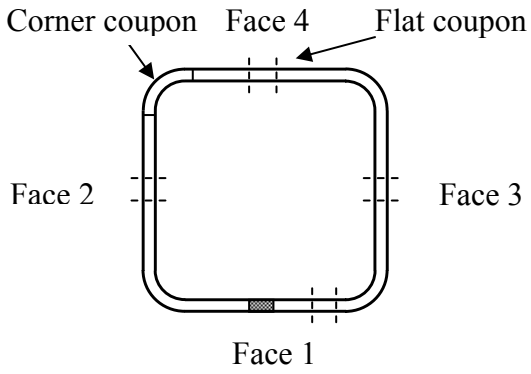

Fig. 2. Face labelling convention

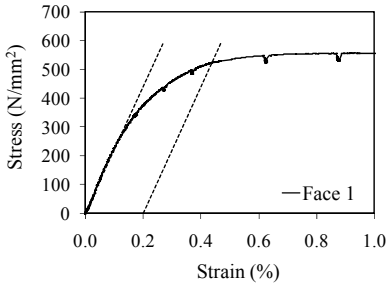

(a) 60×60×3-Face 1

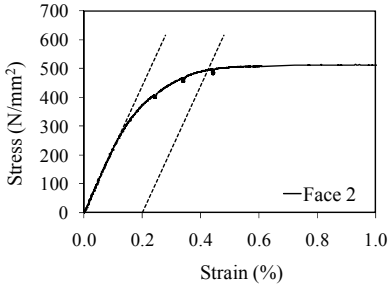

(b) 60×60×3-Face 2

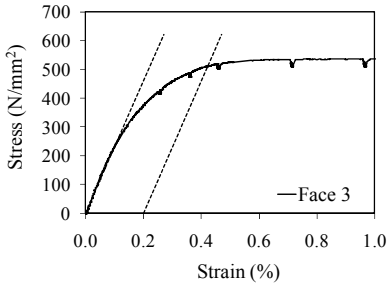

(c) 60×60×3-Face 3

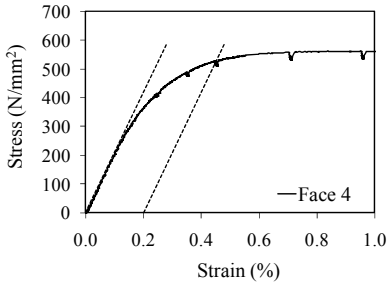

(d) 60×60×3-Face 4

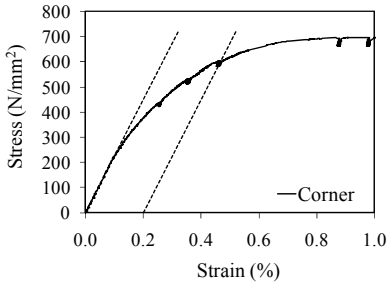

(e) 60×60×3-Corner

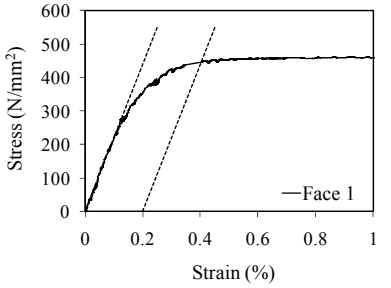

(f) 80×80×3-Face 1

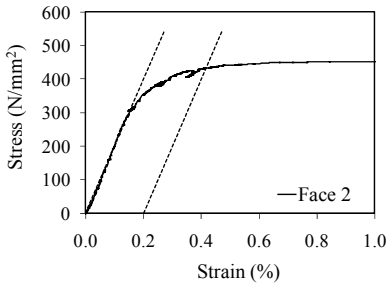

(g) 80×80×3-Face 2

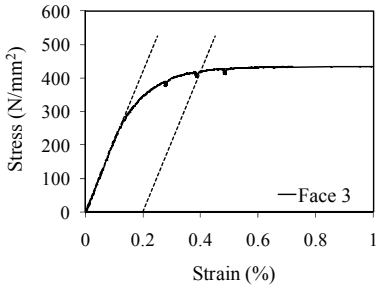

(h) 80×80×3-Face 3

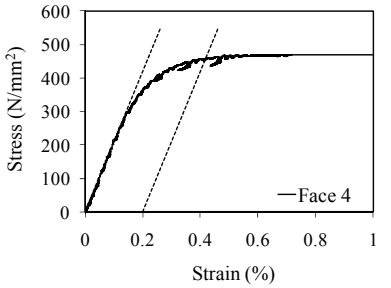

(i) 80×80×3-Face 4

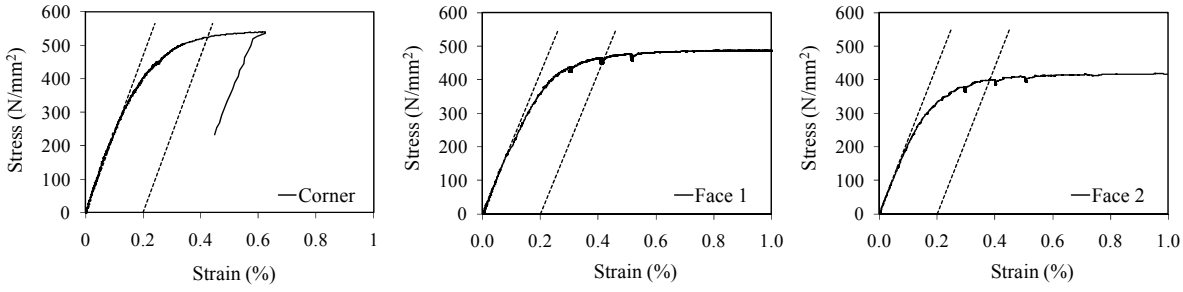

(j) 80×80×3-Corner (k) 120×80×3-Face 1 (l) 120×80×3-Face 2

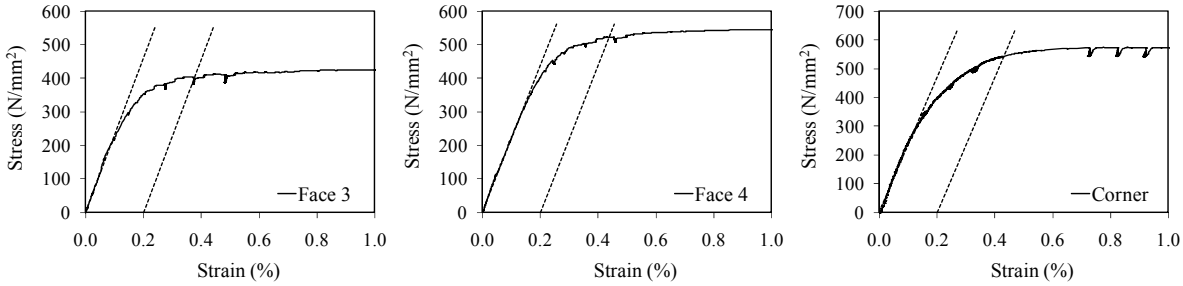

(m) 120×80×3-Face 3 (n) 120×80×3-Face 4 (o) 120×80×3-Corner

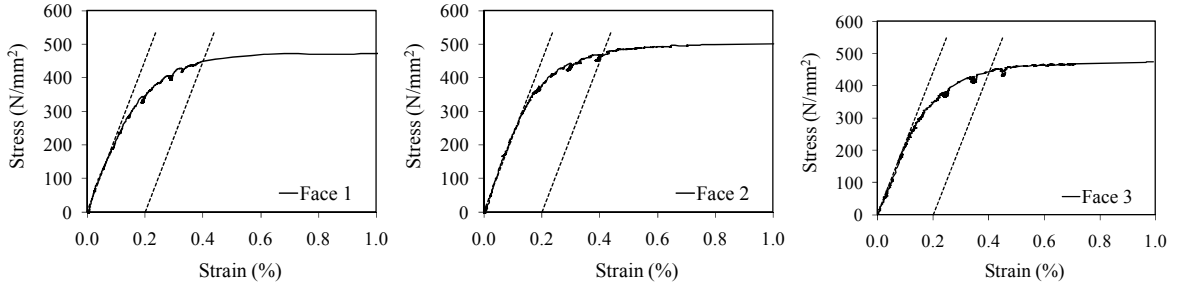

(p) 60×40×3-Face 1 (q) 60×40×3-Face 2 (r) 60×40×3-Face 3

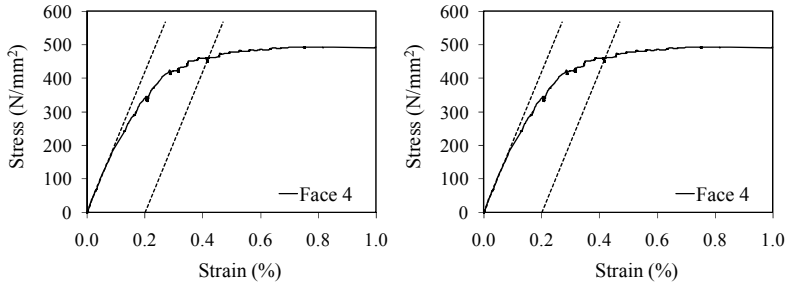

(s) 60×40×3-Face 4 (t) 60×40×3-Corner

Fig. 3. Measured stress-strain curves. (a)-(e) SHS 60×60×3, (f)-(j) SHS 80×80×3, (k)-(o) RHS 120×80×3, (p)-(t) RHS 60×40×3.

2.3. Stub column tests

Stub column tests on four ferritic stainless steel section sizes, RHS 120×80×3, RHS 60×40×3, SHS 80×80×3 and SHS 60×60×3, were performed. Two repeated concentric compression tests were carried out for each section size. Stub column lengths were selected to be short enough to avoid overall flexural buckling, but still long enough to provide a representative pattern of geometric imperfections and residual stresses (Galambos 1998). The chosen nominal lengths were equal to three times the larger nominal cross-section dimension for the RHS 120×80×3, SHS 80×80×3 and SHS 60×60×3 specimens. A shorter length, equal to two times the larger nominal cross-section dimension, was employed for the RHS 60×40×3 specimens, since evidence of global buckling was observed in the failure modes of longer specimens.

The stub column specimens were milled flat and square to ensure a uniform loading distribution during testing and were compressed between parallel platens in an Instron 3500 kN hydraulic testing machine, as shown in Fig. 4. The test set-up was displacement controlled. The average measured geometric dimensions of each stub column specimen are provided in Table 5, where L is the stub column length, h is the section depth, b is the section width, t is the thickness and r_i is the internal corner radius (see Fig. 5). Initial local geometric imperfection magnitudes were not measured specifically to each test specimen, but were measured over a representative 800 mm length of each section size, following the procedures of Schafer and Peköz (1998). The maximum deviations from a flat datum were recorded for the four faces of each section, and then averaged to give the imperfection magnitudes w_0 reported in Table 5.

The ultimate load F_u and the corresponding end shortening at ultimate load δ_u are given in Table 6. All test specimens failed by local buckling of the flat elements comprising the section. Fig. 6 shows a typical failure mode. Tests were continued beyond the ultimate load and the post ultimate response was recorded. Full load-end shortening curves for the tested specimens are depicted in Fig. 7. Relevant guidelines provided by the Centre for Advanced Structural Engineering (1990) were used to eliminate elastic deformation of the end platens from the end shortening measurements. Hence the true deformations of the stub columns were determined and used throughout the study.

Table 5. Measured dimensions of the stub column specimens

Specimen	L (mm)	h (mm)	b (mm)	t (mm)	r_i (mm)	w_0 (mm)	A (mm^2)
RHS 120×80×3-1	362.0	119.9	80.0	2.84	3.70	0.061	1077.9
RHS 120×80×3-2	362.2	120.0	80.0	2.83	3.90	0.061	1074.3
RHS 60×40×3-1	122.1	59.9	40.0	2.81	3.19	0.081	508.1
RHS 60×40×3-2	122.1	59.9	40.0	2.81	3.19	0.081	508.0
SHS 80×80×3-1	242.0	80.1	80.1	2.83	3.67	0.087	850.8
SHS 80×80×3-2	242.0	80.1	80.1	2.82	3.43	0.087	849.1
SHS 60×60×3-1	182.2	60.5	60.5	2.98	2.90	0.061	662.1
SHS 60×60×3-2	182.2	60.5	60.6	2.90	3.10	0.061	654.8

Table 6. Summary of test results for stub columns

Specimen	Ultimate load F_u (kN)	End Shortening at ultimate load δ_u (mm)
RHS 120×80×3-1	449	1.16
RHS 120×80×3-2	441	1.19
RHS 60×40×3-1	278	2.18
RHS 60×40×3-2	271	2.12
SHS 80×80×3-1	392	1.42
SHS 80×80×3-2	389	1.49
SHS 60×60×3-1	376	1.92
SHS 60×60×3-2	370	1.94

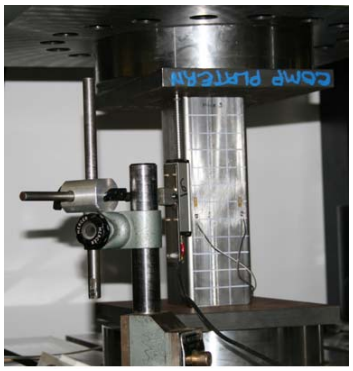

Fig. 4. Stub column testing apparatus

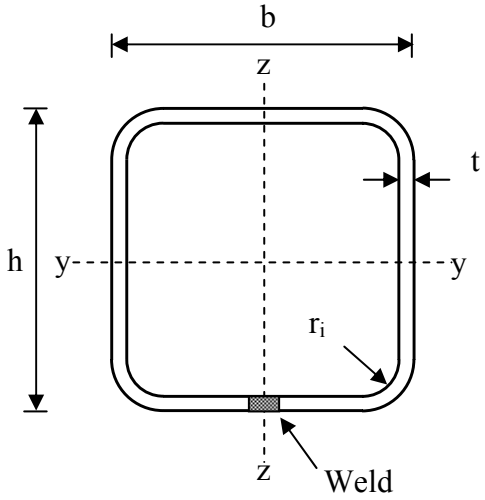

Fig. 5. Face labelling convention

Fig. 6. Typical stub column failure

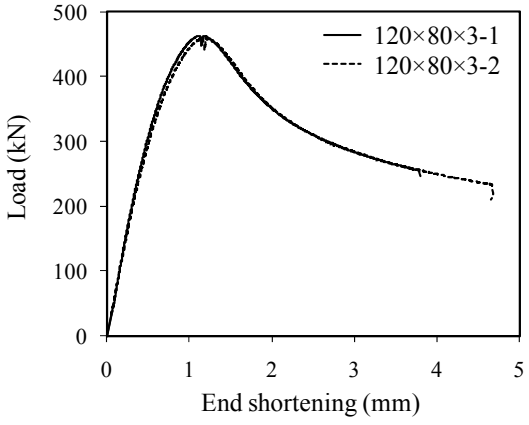

(a) RHS 120×80×3

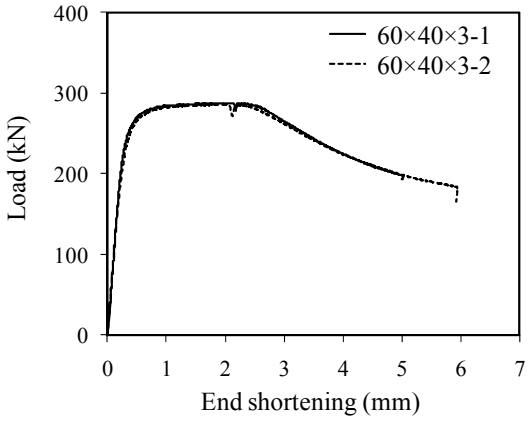

(b) RHS 60×40×3

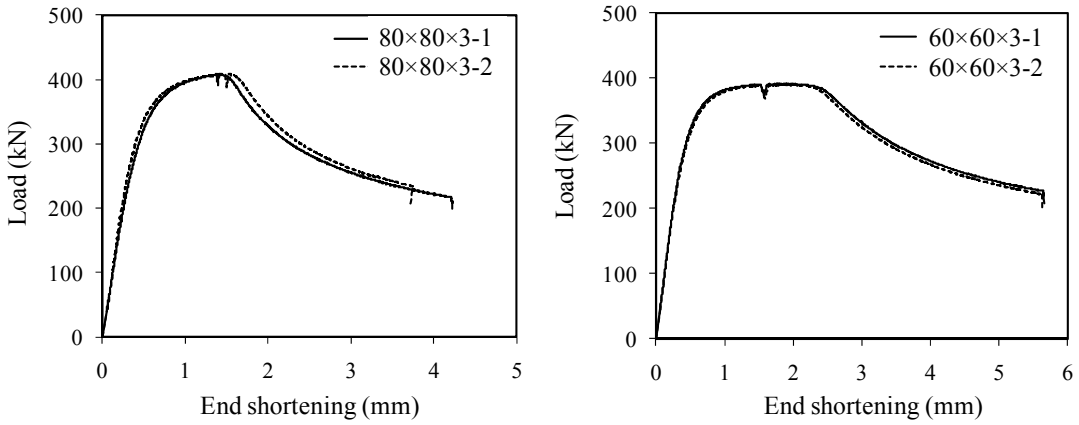

(c) SHS 80×80×3 (d) SHS 60×60×3

Fig. 7. Load-end shortening curves for stub columns

2.4. Beam tests

A total of eight bending tests, in two configurations, were conducted to investigate the cross-section response of SHS and RHS ferritic stainless steel beams under constant moment (four-point bending) and a moment gradient (3-point bending). All specimens had a total length of 1700 mm and were simply supported between two steel rollers, placed 100 mm inwards from the ends of the beams, resulting in a span of 1500 mm. The tested beams were loaded symmetrically, in an Instron 2000 kN hydraulic testing machine, at the third points and at mid-span for the 4-point bending (4PB) and the 3-point bending (3PB) arrangements respectively. Wooden blocks were placed within the tubes at the loading points to prevent web crippling. The test set-up was displacement controlled at a rate of 2 mm/min.

Average measured dimensions of the beam specimens, together with the maximum local imperfections w_0, are reported in Table 7. The ultimate test bending moment M_u and the cross-section rotation capacity R are reported in Table 8. The obtained moment-curvature and mid-span moment-rotation curves from the 4-point and 3-point bending tests are shown in Figs 8 and 9 respectively, where M_u is the ultimate test moment, M_{pl} is the plastic moment capacity, θ is the mid-span rotation, θ_{pl} is the elastic component of the rotation at M_{pl}, κ is the curvature and κ_{pl} is the elastic curvature corresponding to M_{pl}. Rotation capacity was calculated as $R = \kappa_u/\kappa_{pl} - 1$ and $R = \theta_u/\theta_{pl} - 1$ for the 4PB and 3PB tests respectively, where κ_u (θ_u) is the curvature (rotation) at which the moment-curvature (moment-rotation) curve falls below M_{pl} on the descending branch and κ_{pl} (θ_{pl}) is the elastic curvature (rotation) corresponding to M_{pl} on the ascending branch. All test specimens failed by local buckling of the compression flange. Figs 10 and 11 show typical failure modes of the beam specimens from the 4-point and 3-point bending tests respectively.

Table 7. Measured dimensions of the beam specimens

Specimen	L (mm)	h (mm)	b (mm)	t (mm)	r_i (mm)	w_0 (mm)
RHS 120×80×3-4PB	1500	120.0	79.9	2.84	3.78	0.061
RHS 60×40×3-4PB	1500	60.2	39.9	2.86	3.15	0.081
SHS 80×80×3-4PB	1500	80.4	80.0	2.80	3.95	0.087
SHS 60×60×3-4PB	1500	60.7	60.7	2.89	2.86	0.061
RHS 120×80×3-3PB	1500	119.9	79.9	2.83	3.80	0.061
RHS 60×40×3-3PB	1500	60.4	40.8	2.82	3.18	0.081
SHS 80×80×3-3PB	1500	80.5	80.2	2.81	3.81	0.087
SHS 60×60×3-3PB	1500	60.6	60.5	2.87	2.88	0.061

Table 8. Summary of test results for beams

Specimen	Ultimate moment M_u (kNm)	Rotation capacity R
RHS 120×80×3-4pb	20.0	1.45
RHS 60×40×3-4pb	5.3	> 5.00
SHS 80×80×3-4pb	11.3	1.86
SHS 60×60×3-4pb	7.9	3.10
RHS 120×80×3-3pb	21.1	1.30
RHS 60×40×3-3pb	5.9	> 4.18
SHS 80×80×3-3pb	11.4	1.12
SHS 60×60×3-3pb	8.4	2.37

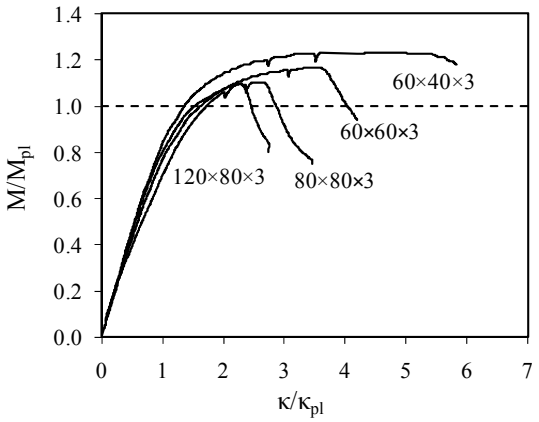

Fig. 8. Normalised moment-curvature response (4-point bending)

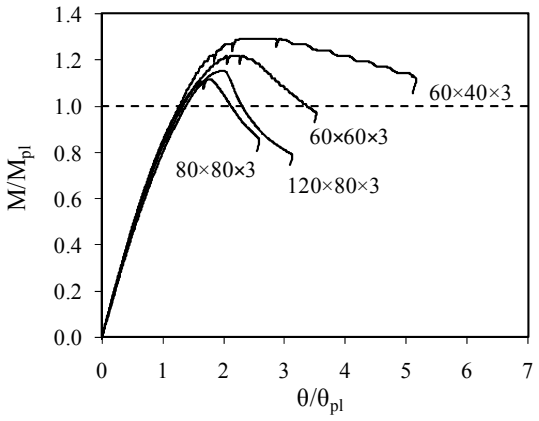

Fig. 9. Normalised moment-rotation response (3-point bending)

Fig. 10. Typical failure mode from 4PB tests

Fig. 11. Typical failure mode from 3PB tests

3. ANALYSIS OF RESULTS AND DESIGN RECOMMENDATIONS

3.1 Cross-section classification

In this section, the experimental results are used to assess the applicability of the cross-section classification limits provided in EN 1993-1-4 (2006) and the proposed limits of Gardner and Theofanous (2008) to ferritic stainless steel internal elements. The measured weighted average material properties from the flat tensile coupon tests for each cross-section were utilised throughout the analyses.

Both the stub column tests results and the bending tests results have been utilised to assess the suitability of the Class 3 slenderness limit for internal elements in compression. Figs 12 and 13 show the relevant response characteristics ($F_u/ A\sigma_{0.2}$ and M_u/ M_{el}), where F_u and M_u are the ultimate test load and moment respectively and M_{el} is the conventional elastic moment capacity, plotted against the slenderness parameter $c/t\varepsilon$ of the most slender constituent element in the cross-section, where c is the compressed flat width, t is the element thickness and $\varepsilon = [(235/f_y)(E/210000)]^{0.5}$ as defined in EN 1993-1-4 (2006). In determining the element slenderness, due account of the stress distribution and element support conditions have been made through the buckling factor k_σ, as defined in EN 1993-1-5 (2006). It may be concluded that the current Class 3 limit given in EN 1993-1-4 (2006) is applicable to ferritic stainless steel internal elements under compression, while the proposed limit of Gardner and Theofanous (2008) allows more efficient exploitation of the material.

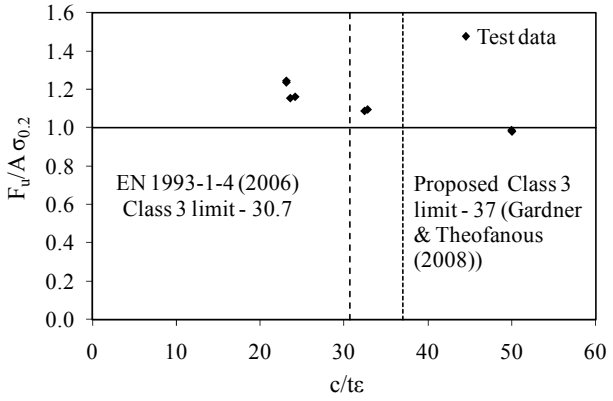

Fig. 12. Assessment of Class 3 slenderness limits for internal elements in compression (from stub column tests)

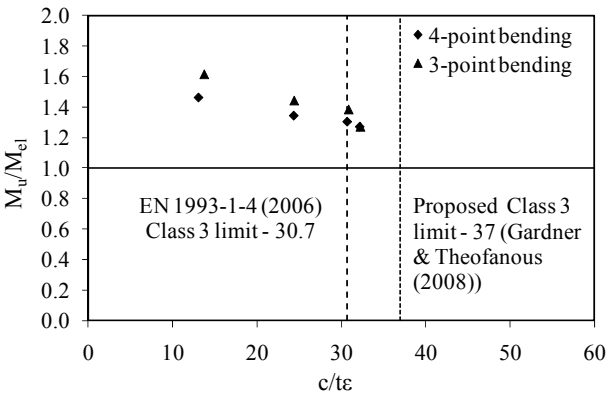

Fig. 13. Assessment of Class 3 slenderness limits for internal elements in compression (from bending tests)

The Class 2 slenderness limits specified in EN 1993-1-4 (2006) and proposed by Gardner and Theofanous (2008), together with the test results are shown in Fig. 14, where the test ultimate moment capacity M_u has been normalised by the plastic moment capacity M_{pl}. In Fig. 15, the rotation capacity R is plotted against the slenderness parameter c/tε of the most slender constituent element in the cross-section. In the absence of a codified deformation capacity requirement for Class 1 stainless steel cross-sections, the equivalent carbon steel rotation capacity requirement of R = 3 (Sedlacek and Feldmann 1995) has been used herein. The EN 1993-1-4 (2006) Class 2 limit of 26.7 may be seen as safe whereas the proposed limit of 35 (Gardner and Theofanous 2008) provides more economical structural design. The Class 1 limit proposed by Gardner and Theofanous (2008) appears optimistic for ferritic stainless steel and the EN 1993-1-4 (2006) provisions may be adopted.

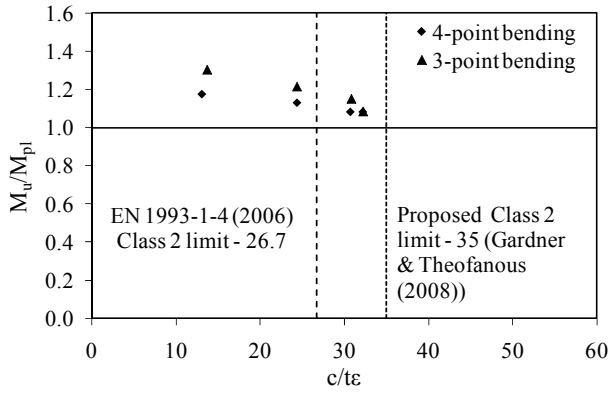

Fig. 14. Assessment of Class 2 slenderness limits for internal compression elements

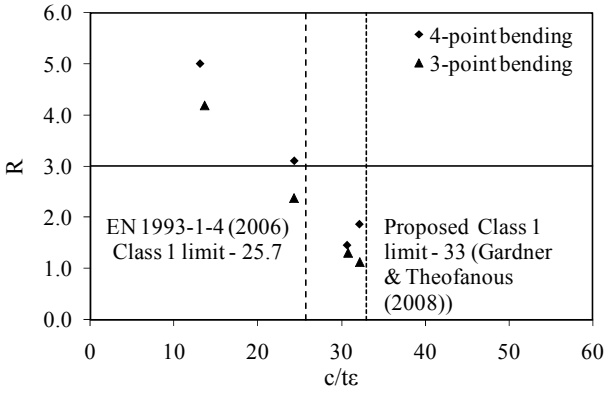

Fig. 15. Assessment of Class 1 slenderness limits for internal compression elements

3.2 Comparison with other stainless steel grades

Test data collected from the literature (Rasmussen and Hancock 1993a, Rasmussen and Hancock 1993b, Talja and Salmi 1995, Kuwamura 2003, Young and Liu 2003, Liu and Young 2003, Gardner and Nethercot 2004a, Gardner and Nethercot 2004b, Young and Lui 2005, Real and Mirambell 2005, Zhou and Young 2005, Gardner at el. 2006, Theofanous and Gardner 2009, Theofanous and Gardner 2010) on austenitic, duplex and lean duplex stainless steel SHS and RHS specimens have been utilised to compare with the test results generated herein and to assess the relative performance of various stainless steel grades. In Fig. 16, the reported ultimate load capacity from stub column tests have been normalised by the respective cross-sectional area and plotted against the c/t ratio of the most slender constituent element in the cross-section The bending tests results reported herein were also compared to tests on other stainless steel grades as shown in Fig. 17, where the ultimate moment capacity normalised by the respective plastic section modulus is plotted against the c/t ratio of the most slender constituent element in the cross-section. The experimental data presented in Figs 16 and 17 exhibit the general anticipated trend of reducing failure stress with increasing slenderness. The vertical scatter for a given slenderness reflects the variation in material strength between the tested specimens. Overall, of the grades considered, lean duplex specimens generally show the

highest failure stress, which is in line with the high yield strength associated with this material, while the results of the other grades overlap.

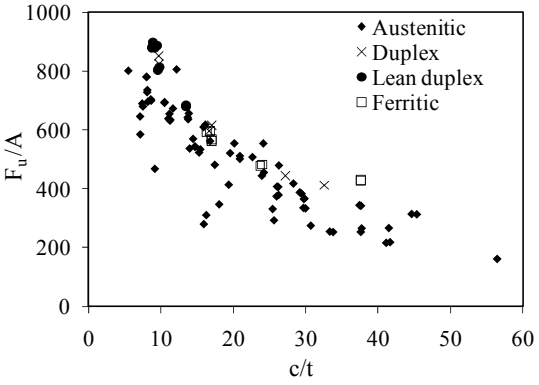

Fig 16. Performance of stub columns of various stainless steel grades

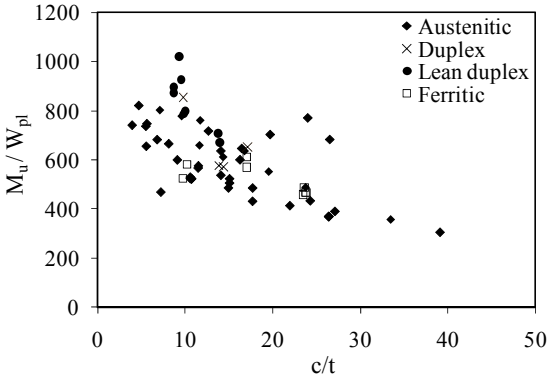

Fig 17. Performance of beams of various stainless steel grades

5. CONCLUSIONS

A laboratory testing programme has been conducted at Imperial College London to investigate the structural performance of ferritic stainless steel tubular structural elements. Eight stub column tests, eight beam tests and a total of twenty material tests have been reported herein. The experimental results were used to assess the provisions of Eurocode 3: Part 1.4 for classification of ferritic stainless steel tubular sections. It was concluded that the current Class 2 and Class 3 slenderness limits provided in EN 1993-1-4 (2006) are applicable to ferritic stainless steel internal elements under compression, while the proposed limits of Gardner and Theofanous (2008) allow greater design efficiency. The Class 1 limit proposed by Gardner and Theofanous (2008) appeared to be unsafe for ferritic stainless steel; hence, the EN 1993-1-4 (2006) limit was recommended. The laboratory test results on ferritic stainless steel were also compared to test results on austenitic, duplex and lean duplex stainless steel SHS and RHS specimens collected from the literature. Overall, ferritic stainless steel shows similar performance to other stainless steel grades and at a lower material cost, making it an attractive choice for structural applications.

ACKNOWLEDGEMENTS

The authors are grateful to the Outokumpu Research Foundation and the Steel Construction Institute for their financial contributions to the project and would like to thank Gordon Herbert and Angeliki Ntikmpasani for their assistance during the experimental investigations.

REFERENCES

Ashraf, M., Gardner, L. and Nethercot, D.A. (2005), "Strength enhancement of the corner regions of stainless steel cross-sections". *J. Construct. Steel Res.,* Vol. **61**(1), 37-52.

Centre for Advanced Structural Engineering. (1990), "Compression tests of stainless steel tubular columns". Investigation Report S770. University of Sydney.

EN 1993-1-4. (2006), Eurocode 3: Design of steel structures - Part 1.4: General rules-Supplementary rules for stainless steel. CEN.

EN 10002-1. (2001), Metallic materials - Tensile testing - Part 1: Method of test at ambient temperature. CEN.
EN 1993-1-5. (2006), Eurocode 3. Design of Steel Structures: Part 1.5: Plated structural elements. CEN.
EN 10088-4. (2009), Stainless steels - Part 4: Technical delivery conditions for sheet/plate and strip of corrosion resisting steels for general purposes. CEN.
Galambos, TV. (1998), *Guide to Stability Design Criteria for Metal Structures.* 5th ed. New York: J. Wiley & Sons.
Gardner, L. and Theofanous, M. (2008), "Discrete and continuous treatment of local buckling in stainless steel elements". *J. Construct. Steel Res.,*Vol. **64**(11), 1207-1216.
Gardner, L. and Nethercot, D.A. (2004a), "Experiments on stainless steel hollow sections-Part 1: Material and cross- sectional behaviour". *J. Construct. Steel Res.,* Vol. **60**(9), 1291-1318.
Gardner, L. and Nethercot, D.A. (2004b), "Experiments on stainless steel hollow sections, Part 2: Member behaviour of columns and beams". *J. Construct. Steel Res.,* Vol. **60**(9), 1319–1332.
Gardner, L. Talja, A. and Baddoo, N.R. (2006), "Structural design of high-strength austenitic stainless steel". *Thin-Walled Struct.,* Vol. **44**(5), 517-528.
Gardner, L. and Theofanous, M. (2010), "Plastic Design of Stainless Steel Structures". *Proceedings of Stability and Ductility of Steel Structures Conference.,* Rio de Janeiro, Brazil.
Kuwamura, H. (2003), "Local buckling of thin-walled stainless steel members". *Steel Structures.,* Vol. **3**(3), 191–201.
Liu, Y. and Young, B. (2003), "Buckling of stainless steel square hollow section compression members". *J. Construct. Steel Res*., Vol. **59**(2), 165-177.
Rasmussen, K.J.R. and Hancock, G.J. (1993a), "Design of cold-formed stainless steel tubular members. I: Columns". *J. Struct. Eng, ASCE.,* Vol. **119**(8), 2349–2367.
Rasmussen, K.J.R. and Hancock, G.J. (1993b), "Design of cold-formed stainless steel tubular members II: Beams". *J. Struct. Eng, ASCE*., Vol. **119**(8), 2368–2386.
Real, E. and Mirambell, E. (2005), "Flexural behaviour of stainless steel beams". *Eng. Struct.,* Vol. **27**(10), 1465–1475.
Sedlacek, G. And Feldmann, M. (1995), The b/t-ratios controlling the applicability of analysis models in Eurocode 3, Part 1.1. Background Document 5.09 for chapter 5 of Eurocode 3, Part 1.1, Aachen.
Schafer, B.W. and Peköz, T. (1998), "Computational modeling of cold-formed steel: characterizing geometric imperfections and residual stresses". *J. Construct. Steel Res.,* Vol. **47**(3), 193-210.
Talja, A. and Salmi, P. (1995), Design of stainless steel RHS beams, columns and beam-columns. Research note 1619. Finland: VTT building technology.
Theofanous, M. and Gardner, L. (2010), "Experimental and numerical studies of lean duplex stainless steel beams". *J. Construct. Steel Res.,* Vol. **66**(6), 816-825.
Theofanous, M. and Gardner, L. (2009), "Testing and numerical modelling of lean duplex stainless steel hollow section columns". *Eng. Struct.,* Vol. **31**(12), 3047-3058.
Young, B. and Liu, Y. (2003), "Experimental investigation of cold-formed stainless steel columns". *J. Struct. Eng, ASCE.,* Vol. **129**(2), 169-176.
Young, B. and Lui, W.M. (2005), "Behaviour of cold-formed high strength stainless steel sections". *J. Struct. Eng, ASCE*., Vol. **131**(11), 1738-1745.
Zhou, F. and Young, B. (2005), "Tests of cold-formed stainless steel tubular flexural members". *Thin-Walled Struct*., Vol. **43**(9), 1325–1337.